Induction of ferroptosis by SIRT1 knockdown alleviates cytarabine resistance in acute myeloid leukemia by activating the HMGB1/ACSL4 pathway

QIAN KONG[1*], QIXIANG LIANG[2*], YINLI TAN[1*], XIANGQIN LUO[1], YESHENG LING[1], XIAOFENG LI[1], YUN CAI[1] and HUIQIN CHEN[1]

[1]Department of Pediatrics, The Third Affiliated Hospital of Sun Yat-sen University, Guangzhou, Guangdong 510000, P.R. China; [2]Department of Stomatology, The Third Affiliated Hospital of Sun Yat-Sen University, Guangzhou, Guangdong 510000, P.R. China

Received June 14, 2024; Accepted September 19, 2024

DOI: 10.3892/ijo.2024.5708

Abstract. Resistance to cytarabine is a major obstacle to the successful treatment of acute myeloid leukemia (AML). The present study aimed to explore the mechanism by which sirtuin 1 (SIRT1) reverses the cytarabine resistance of leukemia cells. Cell viability was investigated using the EdU proliferation assay. The expression levels of molecules were determined by reverse transcription-quantitative PCR, western blotting, and immunofluorescence staining. Flow cytometry was used to detect reactive oxygen species and apoptosis levels, The levels of superoxide dismutase, glutathione and malondialdehyde were examined by ELISA. Mitochondrial damage was investigated by transmission electron microscopy. Furthermore, tumor growth was evaluated in a xenograft model. The results revealed that SIRT1 expression was significantly upregulated in drug-resistant leukemia cells. By contrast, knockdown of SIRT1 reversed cytarabine resistance in HL60 cells by promoting ferroptosis. Mechanistically, SIRT1 could regulate the translocation of HMGB1 from the nucleus to the cytoplasm in cytarabine-resistant HL60 (HL60/C) cells. Furthermore, knockdown of HMGB1 inhibited the expression of ACSL4. In addition, knockdown of SIRT1 expression could inhibit the growth of HL60/C cells *in vivo* and reverse cytarabine resistance. In conclusion, the present results demonstrated that SIRT1 inhibition could be a promising strategy to overcome cytarabine resistance in AML.

Correspondence to: Dr Huiqin Chen or Dr Yun Cai, Department of Pediatrics, The Third Affiliated Hospital of Sun Yat-sen University, 600 Tianhe Road, Guangzhou, Guangdong 510000, P.R. China
E-mail: chenhuiqin0101@163.com
E-mail: caiyun@mail.sysu.edu.cn

*Contributed equally

Abbreviations: AML, acute myeloid leukemia; HMGB1, high mobility group box-1 protein; CCK-8, Cell Counting Kit-8; ROS, reactive oxygen species

Key words: acute myeloid leukemia, sirtuin 1, HMGB1, ferroptosis, resistance

Introduction

Acute myeloid leukemia (AML) is a type of tumor that affects stem cell precursors of the myeloid lineage, including red blood cells, platelets and white blood cells (1,2). The development of AML is caused by genetic mutations such as familial mutations in CEBPA, DDX4 and RUNX1 genes, resulting in uncontrolled proliferation and hematopoietic stem cell abnormalities (1,2). Among adults, AML is the second most common form of leukemia worldwide and the 5-year survival rate is <30% (3). Cytarabine is the first-line drug used to treat AML. Although cytarabine-based regimens can induce a complete response in most newly diagnosed patients with AML, the overall clinical outcome remains unsatisfactory due to drug resistance (4). Therefore, it is crucial to develop strategies to overcome drug resistance.

Multiple mechanisms, including apoptosis, autophagy and ferroptosis, have been suggested to be involved in drug resistance (5-7). Ferroptosis is a distinct iron-dependent form of cell death that differs from apoptosis, necrosis and autophagy (8). It has been reported that enhancing ferroptosis can reverse drug resistance and improve cancer treatment (9). For example, it has been shown that the use of ferroptosis inducers can synergistically sensitize ovarian cancer cells to a PARP inhibitor (10). Liu *et al* (11) demonstrated that enhancing ferroptosis by impairing STAT3-Nrf2-glutathione peroxidase 4 (GPX4) signaling could increase the sensitivity of osteosarcoma cells to cisplatin. Notably, it has also been suggested that inducing ferroptosis can reverse the resistance of cytarabine in AML (12); however, the underlying mechanism has yet to be fully elucidated.

Sirtuin 1 (SIRT1) is a member of the class III family of NAD(+)-dependent histone deacetylases, which serves an important role in various cellular processes, such as cell proliferation, apoptosis, inflammation, oxidation response and drug resistance (13,14). Previous studies have shown that SIRT1 contributes to drug resistance by deacetylating its downstream targets, such as FOXO3 and WEE1 (15,16). In addition, SIRT1

upregulation by cytarabine has been reported to be inhibited by Tenovin-6 in acute lymphoblastic leukemia (17). However, the mechanism by which SIRT1 regulates the drug resistance of leukemia cells is currently unclear. High mobility group box-1 protein (HMGB1) is a nuclear DNA-binding protein involved in nucleosome stabilization and gene transcription. In acute kidney injury, cytoplasmic HMGB1 can induce ferroptosis by regulating ACSL4 (18). The present study aimed to explore the effects of SIRT1 knockdown on the induction of ferroptosis via the HMGB1/ACSL4 pathway, which may reverse cytarabine resistance in AML. The present findings demonstrated that SIRT1 inhibition could be a promising strategy to overcome cytarabine resistance.

Materials and methods

Cell culture and reagents. The leukemia cell lines HL60, K562 and Kasumi-1 (Kas-1) were purchased from Procell Life Science & Technology Co., Ltd. HL60 and Kas-1 cells were isolated from AML, whereas K562 cells were isolated from chronic myeloid leukemia. Cells were maintained in RPMI 1640 medium (Gibco; Thermo Fisher Scientific, Inc.) supplemented with 10% fetal bovine serum (Gibco; Thermo Fisher Scientific, Inc.), 1% 100 U/ml penicillin G and 100 mg/ml streptomycin. Cells were cultured at 37˚C with 5% CO_2. Cytarabine was purchased from MilliporeSigma. Drug-resistant leukemia cell lines were established as described previously (19). Briefly, 10^5 cells were inoculated into a 6-well plate, and when cells reached 80% confluence, different concentrations (0, 1, 2, 5 and 10 μmol) of cytarabine were added. Subsequently, the medium was changed every 3-4 days for 3-4 weeks. The IC_{50} concentrations of cytarabine in HL60, K562 and Kas-1 cells were 5 μmol, 100 nmol and 50 nmol, respectively.

Small interfering RNA (siRNA) transfection. SIRT1, HMGB1, ACSL4 and negative control (NC) siRNA sequences were obtained from Shanghai GenePharma Co., Ltd. siRNA transfection was performed using Lipofectamine® 3000 (Invitrogen; Thermo Fisher Scientific, Inc.) according to the manufacturer's instructions. Briefly, 10^5 cytarabine-resistant HL60 (HL60/C) cells or HL60 cells were inoculated into a 6-well plate and were grown to 40-50% confluence. Subsequently, 50 nmol siRNA was diluted in Opti-MEM (Thermo Fisher Scientific, Inc.), mixed with 2 μl Lipofectamine 3000, added to the cell culture plate and cultured for 48 h at 37˚C with 5% CO_2. The siRNA sequences were as follows: si-SIRT1, forward 5'-GUGGCAGAUUGUUAUUAAUTT-3', reverse 5'-AUUAAUAACAAUCUGCCACTT-3'; si-SIRT1-2, forward 5'-UUCUGAAAUAUUCAAUAUCAA-3', reverse 5'-GAUAUUGAAUAUUUCAGAAAA-3'; si-SIRT1-3, forward 5'-UUUUCCUUCCUUAUCUGACAA-3', reverse 5'-GUCAGAUAAGGAAGGAAAACU-3'; si-HMGB1-1, forward 5'-GCUCAAGGAGAAUUUGUAATT-3', reverse 5'-UUACAAAUUCUCCUUGAGCTT-3'; si-HMGB1-2,forward 5'-ACAAAAAAUGCAUAUGAUGAC-3', reverse5'-CAUCAUAUGCAUUUUUUGUGC-3'; si-HMGB1-3, forward 5'-AGUUUCUUCGCAACAUCACCA-3', reverse 5'-GUGAUGUUGCGAAGAAACUGG-3'; si-ACSL4-1, forward 5'-GAUGGAUGCUUACAGAUUA-3', reverse 5'-UAAUCUGUAAGCAUCCAUC-3'; si-ACSL4-2, forward 5'-AUAUUGUUAUUAACAAGUGGA-3', reverse 5'-CACUUGUUAAUAACAAUAUAC-3'; si-ACSL4-3,forward 5'-ACUGUAUAUUGUUAUUAACAA-3', reverse 5'-GUUAAUAACAAUAUACAGUGC-3'; si-NC, forward 5'-UUCUCCGAACGUGUCACGUTT-3' and reverse, 5'-ACGUGACACGUUCGGAGAATT-3'.

Co-immunoprecipitation (IP) assay. The possible protein interaction network of SIRT1 was constructed using the STRING database (https://string-db.org/).The SIRT1-HA and HMGB1-Flag overexpression vectors were constructed using pcDNA3.1 plasmids (Beyotime Institute of Biotechnology). Briefly, 1 μg SIRT1-HA and HMGB1-Flag vectors were diluted in Opti-MEM, mixed with 2 μl Lipofectamine 3000 and transfected into 293T (Procell Life Science & Technology Co., Ltd.), HL60 and HL60/C cells. After culturing at 37˚C for 24 h, the cells were collected and added to 100 μl RIPA lysis buffer (Beyotime Institute of Biotechnology) on ice for 30 min, and the supernatant was collected by centrifugation at 10,000 x g for 10 min at 4˚C. Subsequently, 5 μg anti-Flag (cat. no. AE063; ABclonal Biotech Co., Ltd.) and anti-HA (cat. no. AE105; ABclonal Biotech Co., Ltd.) antibodies were added to the protein A/G agarose beads (Beyotime Institute of Biotechnology) and incubated at 4˚C overnight. Next, the 10 μl antibody-protein A/G agarose bead complex was added to the cell lysate and slowly shaken at 4˚C for 2-4 h to conjugate the antibody to the protein A/G agarose beads. After the immunoprecipitation reaction, the agarose beads were centrifuged at 1,500 x g at 4˚C for 3 min and the precipitation was collected. The agarose beads were washed with 1 ml RIPA lysis buffer (Beyotime Institute of Biotechnology) 3-4 times. Finally, SDS loading buffer was added for western blot analysis.

Cell viability analysis. The Cell Counting Kit-8 (CCK-8; Dojindo Molecular Technologies, Inc.) was used to determine cell viability. AML cells ($5x10^4$/well) were plated in 96-well plates and treated with cytarabine (5 μmol) at 37˚C for 24 h. Subsequently, 10 μl CCK-8 solution was added to each well and the cells were incubated at 37˚C for 2-3 h. The absorbance was measured at 450 nm using a microplate reader.

EdU proliferation assay. Cells were transfected with si-NC or si-SIRT1 and were treated with cytarabine (5 μmol) at 37˚C for 24 h. Cells ($5x10^4$ cells/well) were then plated in 24-well plates, washed with PBS and incubated in serum-free medium containing 10 μmol/l EdU (Guangzhou RiboBio Co., Ltd.) for 2 h at 37˚C. Cells were fixed in 4% paraformaldehyde (Beyotime Institute of Biotechnology) for 15 min at 4˚C, after which, they were stained with Apollo solution and DNA staining solution (Beyotime Institute of Biotechnology) at room temperature. Images of the cells were then captured using a fluorescence microscope (Nikon Corporation).

Apoptosis analysis. AML cells ($5x10^4$/well) were plated in 24-well plates and treated with cytarabine (5 μmol) at 37˚C for 24 h. Flow cytometric analysis was subsequently performed using the Annexin V-FITC kit (Beyotime Institute of Biotechnology) according to the manufacturer's instructions. Apoptotic cells were analyzed by flow cytometry (LSRFortessa; BD Biosciences) and FlowJo-V10 software (FlowJo, LLC) was used to process the experimental results.

Determination of reactive oxygen species (ROS). The intracellular ROS production in AML cells was determined using the 2',7'-dichlorofluorescein diacetate (DCFH-DA) probe. Briefly, cells were harvested and washed with serum-free medium, after which, they were incubated with 10 μM DCFH-DA diluted in serum-free medium at 37˚C for 30 min. Subsequently, the cells were washed with serum-free medium to remove the unbound DCFH-DA probe, and fluorescence-labeled cells were analyzed by flow cytometry (LSRFortessa; BD Biosciences) and FlowJo-V10 software was used to process the experimental results.

Reverse transcription-quantitative PCR (RT-qPCR). After treatment, total RNA was isolated from AML cells using TRIzol® reagent (Invitrogen; Thermo Fisher Scientific, Inc) and was reverse transcribed into cDNA using PrimeScript™ RT Master Mix (Takara Biotechnology Co., Ltd.) according to the manufacturer's instructions. qPCR was performed using the Fast SYBR Green Master Mix (Thermo Fisher Scientific, Inc.) on a 7900 Real-Time PCR System (Applied Biosystems; Thermo Fisher Scientific, Inc.). The qPCR conditions were as follows: 95˚C for 10 min, followed by 35 cycles at 94˚C for 30 sec, 60˚C for 15 sec and 72˚C for 30 sec. Relative mRNA expression was calculated using the $2^{-\Delta\Delta Cq}$ method (20). GAPDH was used as the internal control. The primer sequences were as follows: HMGB1, forward 5'-TAACTAAACATGGGCAAAGGAG-3', reverse 5'-TAGCAGACATGGTCTTCCAC-3'; SIRT1, forward 5'-TAGCCTTGTCAGATAAGGAAGGA-3', reverse 5'- ACAGCTTCACAGTCAACTTTGT-3'; GAPDH, forward 5'-GCACCGTCAAGGCTGAGAAC-3' and reverse 5'-TGGTGAAGACGCCAGTGGA-3'.

Immunofluorescence staining. AML cells were fixed in 4% formaldehyde at 4˚C for 20 min followed by permeabilization with 0.1% Triton X-100 at room temperature for 10 min. The cells were then washed three times with PBS, blocked with 5% bovine serum albumin (Beyotime Institute of Biotechnology) for 30 min at room temperature, and incubated overnight at 4˚C with anti-GPX4 (1:1,000; cat. no. A11243), anti-HMGB1 (1:1,000; cat. no. A2553) and anti-SIRT1 (1:1,000; cat. no. A11267) (all from ABclonal Biotech Co., Ltd.), followed by incubation with CoraLite 488-conjugated secondary antibody (1:200; cat no. SA00013-2; Wuhan Sanying Biotechnology). The nuclei were stained with DAPI at room temperature for 5 min. Cells were visualized using a confocal microscope (Olympus Corporation).

Western blot analysis. After treatment, AML cells were collected and lysed in RIPA lysis buffer (Beyotime Institute of Biotechnology). The lysates were incubated on ice for 20 min and centrifuged at 10,000 x g for 30 min at 4˚C, before the protein concentration was determined using a BCA kit (Beyotime Institute of Biotechnology). Protein samples (20 μg) were separated by SDS-PAGE on 10% gels and were transferred onto polyvinylidene difluoride membranes (MilliporeSigma). The membranes were blocked with 5% non-fat dry milk diluted in Tris-buffered saline-0.5% Tween-20. Subsequently, the membranes were incubated with anti-SIRT1 (1:1,000; cat. no. A11267), anti-GPX4 (1:1,000, cat. no. A11243), anti-HMGB1 (1:1,000; cat. no. A2553),anti-ACSL4 (1:1,000; cat. no. A20414) and anti-GAPDH (1:5,000; cat. no. A19056) (all from ABclonal Biotech Co., Ltd.) overnight at 4˚C. After three washes, the membranes were incubated with a HRP-conjugated secondary antibody (1:10,000; cat. no. AS014; ABclonal Biotech Co., Ltd.) for 60 min at room temperature. Protein bands were visualized using a chemiluminescence imaging system (Tanon-4600; Tanon Science and Technology Co., Ltd.) and ImageJ 1.8.0.345 software (National Institutes of Health) was used for gray value analysis.

Measurements of superoxide dismutase (SOD), glutathione (GSH) and malondialdehyde (MDA). AML cells were collected and lysed in RIPA lysis buffer (Beyotime Institute of Biotechnology). The MDA, GSH and SOD levels in cell lysates were measured using MDA (cat. no. ab287797; Abcam), GSH (cat. no. E-EL-0026; Wuhan Elabscience Biotechnology Co., Ltd.) and SOD assay kits (cat. no. ab316899;Abcam) according to the manufacturers' instructions.

Xenograft assay. A total of 15 nude mice (male; age, 7-8 weeks; weight, 20-22 g) were purchased from the Guangzhou Ruige Biological Technology Co., Ltd. The mice were raised under pathogen-free conditions (temperature: 20-26˚C; humidity: 40-70%) with a 12-h light/dark cycle, and had free access to water and food.

For *in vivo* imaging, 9 nude mice were randomly divided into three groups: Control, si-NC and si-SIRT1 (n=3). Briefly, $2x10^6$ HL60/C cells transfected with si-NC or si-SIRT1 were resuspended in 100 μl Matrigel (cat. no. 356234; Corning, Inc.) and were injected into the dorsal flanks right of the midline of nude mice. Meanwhile, the same operation with $2x10^6$ HL60 cells was performed in the control group. The mice were observed every day. At day 7, mice were intraperitoneally injected with cytarabine (20 mg/kg, three times a week) for 2 weeks. The mice in all groups underwent a luciferase activity assay. Briefly, anesthesia was induced by 2-3% isoflurane inhalation and was maintained using 1.5-2% isoflurane. The mice were intraperitoneally injected with luciferin potassium salt (150 mg/kg; Shanghai Yeasen Biotechnology Co., Ltd.)and luciferase was detected after 30 min using a live animal imaging system (AniView100; Guangzhou Boluteng Biotechnology Co., Ltd.). Subsequently, these 9 mice were euthanized by cervical dislocation.

In addition, another xenograft assay was conducted. A total of 6 nude mice were randomly divided into two groups: si-NC and si-SIRT1 (n=3); $2x10^6$ HL60/C cells transfected with si-NC or si-SIRT1 were resuspended in 100 μl Matrigel and were injected into the dorsal flanks right of the midline of nude mice (n=3). At day 7, mice were intraperitoneally injected with cytarabine (20 mg/kg, three times a week) for 2 weeks. The tumor growth was observed continuously for 21 days. Prior to sacrifice, 0.2 ml of blood was collected from the orbit of the mice, the blood was left at room temperature for 2 h, centrifuged for 10,000 x g for 5 min at 4˚C and serum was collected; subsequently, these 6 mice were euthanized by cervical dislocation to collect tumor tissue samples before reaching the humane endpoint: Tumor weight did not exceed 10% of body weight.

The animal experiments were performed by Guangzhou Seyotin Biotechnology Co., Ltd. and all experiments were approved by the Animal Ethics Committee of Guangzhou

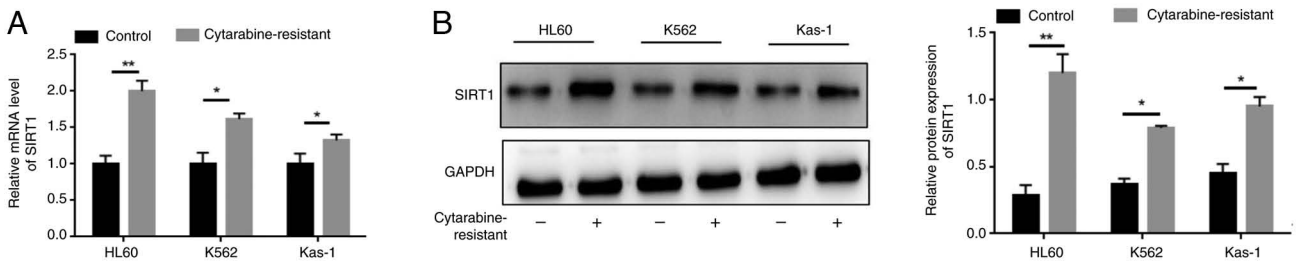

Figure 1. SIRT1 expression is significantly upregulated in Cytarabine-resistant leukemia cells. (A) Reverse transcription-quantitative PCR analysis of the mRNA expression levels of SIRT1 in HL60, K562 and Kas-1 cells. (B) Western blot analysis of SIRT1 in HL60, K562 and Kas-1 cells. *P<0.05, **P<0.01. Kas-1, Kasumi-1; SIRT1, sirtuin 1.

Seyotin Biotechnology Co., Ltd. (approval nos. SYT20203010 and SYT2024079).

Transmission electron microscopy. AML cells were harvested and fixed in 2.5% glutaral-dehyde for 3 h at 4˚C. After three washes with 0.1 M phosphate buffer, the cells were fixed with 1% OsO_4 at room temperature for 2 h. The cells were washed again with 0.1 M phosphate buffer, and were then dehydrated with graded acetone and embedded in Epon resin for 12 h at 37˚C, for 12 h at 45˚C and for 24 h at 60˚C, then sectioned at 50-70 nm with an ultramicrotome. The sections were double stained with 3% uranyl acetate and lead citrate (ddH_2O, 30 ml; lead nitrate, 1.33 g; sodium citrate, 1.76 g) for 30 min at room temperature and observed with a transmission electron microscope (Hitachi, Ltd.).

Isolation of cytoplasmic proteins. After treatment, nuclear and cytoplasmic protein fractions were extracted from HL60/C cells using a Nuclear and Cytoplasmic Protein Extraction Kit (Beyotime Institute of Biotechnology). The protein concentration was measured using a BCA kit (MilliporeSigma). Equal amounts of cytoplasmic proteins were loaded on gels for SDS-PAGE and were transferred to membranes. Western blot analysis was performed with anti-HMGB1,anti-GAPDH and anti-Histone (1:1,000; cat. no. AF0863; Affinity Biosciences).

Statistical analysis. The experiments were repeated three times and all data are presented as the mean ± SD. GraphPad Prism 7 (Dotmatics) was used to analyze and plot the data. Multigroup comparisons were performed using one-way ANOVA followed by the Tukey post hoc multiple comparisons test. Comparisons between two groups were performed using an unpaired Student's t-test. P<0.05 was considered to indicate a statistically significant difference.

Results

SIRT1 expression is significantly upregulated in cytarabine-resistant leukemia cells. To address the involvement of SIRT1 in cytarabine resistance, its expression levels in cytarabine-resistant leukemia cells (HL-60, K562 and Kas-1) were detected. As shown in Figs. 1A and S1, the relative mRNA expression levels of SIRT1, HMGB1and ACSL4 were significantly increased in cytarabine-resistant leukemia cells compared with those in the control group. Similarly, the protein expression levels of SIRT1 in cytarabine-resistant leukemia cells were markedly increased (Fig 1B). Taken together, these findings indicated that SIRT1 may be elevated in cytarabine-resistant leukemia cells.

Knockdown of SIRT1 enhances apoptosis and inhibits proliferation of HL60/C cells treated with cytarabine. To confirm the potential role of SIRT1 in cytarabine-resistant leukemia cells, HL60/C cells were transfected with si-SIRT1 sequences. The knockdown of SIRT1 was confirmed in HL60/C through RT-qPCR (Fig. 2A) and western blot analysis (Fig. 2B). Among the siRNAs, si-SIRT1-1 had the best knockdown effect and was therefore used in subsequent experiments. Furthermore, cell viability was significantly reduced in the si-SIRT1 group (Fig. 2C), and the IC_{50} value was also significantly decreased (Fig. S2). In addition, transfection of si-SIRT1 into HL60 cells was detected by RT-qPCR (Fig. S3A), and knockdown of SIRT1 did not affect the viability of HL60 parental cells (Fig. S3B). The apoptosis rate was significantly increased in the si-SIRT1 group (Fig. 2D)l; however, the apoptosis rate of HL60 parental cells was the highest (Fig. S4). Regarding the rate of apoptosis, Q2 represents late apoptosis and Q3 represents early apoptosis.

Knockdown of SIRT1 enhances the ferroptosis of HL60/C cells. To confirm the potential role of SIRT1 in ferroptosis, HL60/C cells were transfected with si-SIRT1 sequences. The results showed that SOD and glutathione (GSH) activities were decreased, whereas MDA levels were elevated in the si-SIRT1 group compared with those in the si-NC group (Fig. 3A-C). In addition, knockdown of SIRT1 significantly enhanced ROS levels compared with those in the si-NC group (Fig. 3D). It was also observed that knockdown of SIRT1 reduced the expression levels of GPX4 in HL60/C cells (Fig. 3E and G). Moreover, mitochondrial damage is closely associated with ferroptosis, and knockdown of SIRT1 elevated mitochondrial damage in HL60/C cells compared with that in the si-NC group (Fig. 3F). These findings suggested that SIRT1 may serve a critical role in ferroptosis in cytarabine-resistant leukemia cells.

SIRT1 regulates HMGB1 expression and inhibits the cytoplasmic translocation of HMGB1. The possible protein interaction network of SIRT1 was constructed using the STRING database (https://string-db.org/) and it was indicated that SIRT1 may regulate HMGB1 expression (Fig. 4A). Notably, through double immunofluorescence labelling, SIRT1 and HMGB1 were localized. The results showed that SIRT1

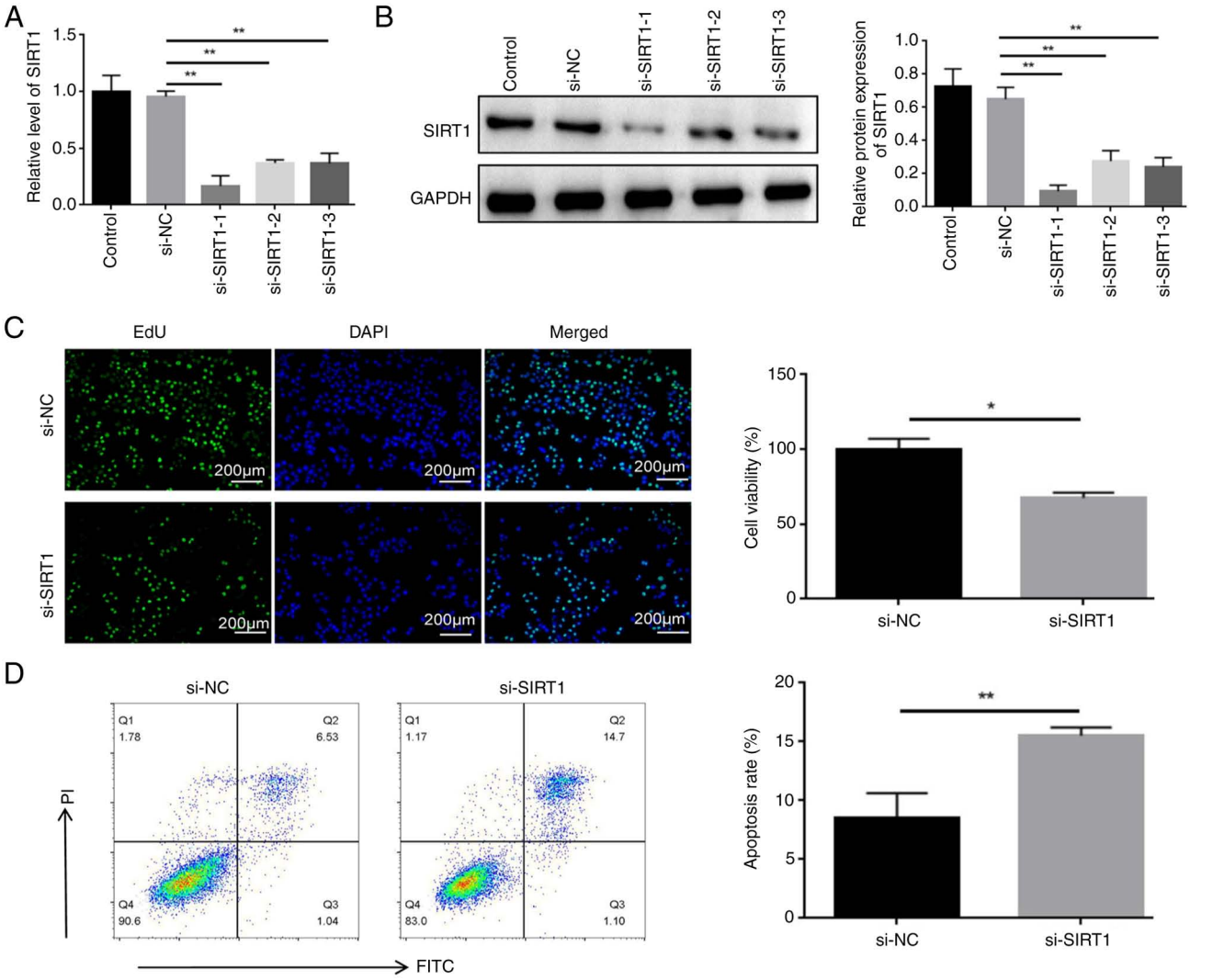

Figure 2. Knockdown of SIRT1 enhances apoptosis and inhibits proliferation of HL60/C cells treated with cytarabine. (A) Reverse transcription-quantitative PCR analysis of the knockdown efficiency of si-SIRT1 sequences. (B) Western blot analysis of the knockdown efficiency of si-SIRT1 sequences. (C) EdU proliferation assay was used to detect the effects of SIRT1 knockdown on the viability of HL60/C cells. (D) Flow cytometry detected the apoptosis rate of HL60/C cells with SIRT1 knockdown. *P<0.05, **P<0.01. HL60/C, cytarabine-resistant HL60; NC, negative control; si, small interfering; SIRT1, sirtuin 1.

and HMGB1 were expressed in the nucleus, with obvious co-localization (Fig. 4B). Subsequently, the overexpression vectors SIRT1-HA and HMGB1-Flag were transfected into 293T, HL60 and HL60/C cells, and the mRNA expression levels of SIRT1 and HMGB1 were significantly upregulated (Figs. S5 and S6). Furthermore, the results of co-immunoprecipitation confirmed the interaction between SIRT1 and HMGB1 in 293T cells (Fig. 4C). In addition, the same results were detected in HL60 and HL60/C cells (Fig. 4D). Notably, it was also observed that si-SIRT1 increased the expression levels of HMGB1 in the cytoplasm and decreased the levels in the nucleus of HL60/C cells. These findings indicated that SIRT1 may interact with HMGB1 and inhibit its cytoplasmic translocation.

Knockdown of HMGB1 reduces the ferroptosis of HL60/C cells. To confirm the potential role of HMGB1 in ferroptosis, HL60/C cells were transfected with si-HMGB1 sequences. The knockdown of HMGB1 was confirmed through RT-qPCR and western blot analysis, and si-HMGB1-1 has the best knockdown effect (Figs. 5A and S7). Subsequently, the results of the EdU proliferation assay showed that the viability of si-HMGB1-1-transfected cells was markedly higher than that in the si-NC group (Fig. 5B). The present study also examined the effects of HMGB1 knockdown on the expression of ferroptosis-related markers. The results showed that knockdown of HMGB1 elevated the activities of SOD, and the levels of GSH and GPX4, compared with those in the si-NC group (Fig. 5C, F and G). By contrast, knockdown of HMGB1 reversed the elevation of MDA and ROS in HL60/C cells (Fig. 5D and E). Taken together, these findings suggested that HMGB1 may induce the ferroptosis of HL60/C cells.

Knockdown of HMGB1 reduces the expression of ACSL4 in HL60/C cells. The present results suggested that, after knockdown of HMGB1, the relative mRNA and protein expression levels of ACSL4 were significantly reduced in HL60/C cells (Fig. 6A and B). To validate the relationship between SIRT1 and ASCL4, and the effect of this pathway on ferroptosis, HL60/C cells were transfected with si-SIRT1 and/or si-ACSL4. As shown

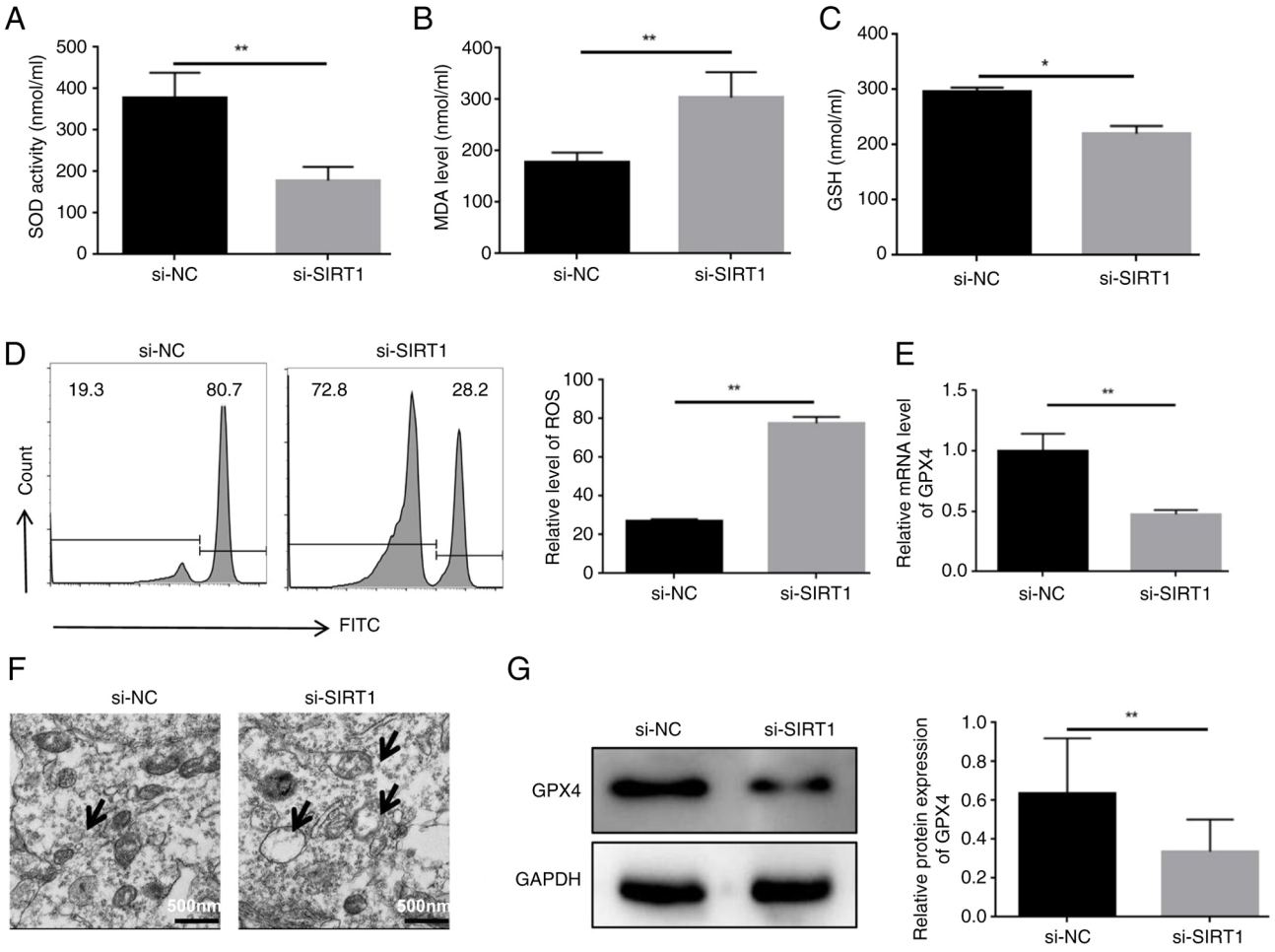

Figure 3. Knockdown of SIRT1 enhances the ferroptosis of HL60/C cells. ELISAs were used to detect the effect of SIRT1 knockdown on (A) SOD, (B) MDA and (C) GSH in HL60/C cells. (D) Flow cytometry detected the impact of SITR1 knockdown on ROS levels in HL60/C cells. (E) mRNA expression levels of GPX4 were detected by reverse transcription-quantitative PCR. (F) Transmission electron microscopy was used to observe mitochondrial damage, as indicated by arrows. (G) Western blot analysis of the effect of SIRT1 knockdown on GPX4 expression in HL60/C cells. *P<0.05, **P<0.01. GPX4, glutathione peroxidase 4; GSH, glutathione; HL60/C, cytarabine-resistant HL60; MDA, malondialdehyde; NC, negative control; ROS, reactive oxygen species; si, small interfering; SIRT1, sirtuin 1; SOD, superoxide dismutase.

in Fig. S8, si-ACSL4 significantly reduced the mRNA expression levels of ACSL4 compared with those in the si-NC group. Notably, it was observed that ROS and MDA levels were markedly increased in HL60/C cells in response to si-SIRT1; however, this effect was counteracted by knocking down ACSL4 (Fig. 6C and D). Similarly, knockdown of SIRT1 decreased SOD activity and relative expression levels of GPX4 in HL60/R cells, but both were elevated in the si-SIRT1 + si-ACSL4 group (Fig. 6E and F). Taken together, these findings suggested that knockdown of SIRT1 may induce the cytoplasmic translocation of HMGB1 and increase ferroptosis through the HMGB1/ACSL4 pathway in HL60/C cells.

Knockdown of SIRT1 blocks the growth of HL60/C cells in vivo. To evaluate whether knockdown of SIRT1 affects the growth of HL60/C cells *in vivo*, *in vivo* imaging was used to observe the size of the tumor. *In vivo* imaging results showed that tumor growth was significantly inhibited in the si-SIRT1 group compared with that in the si-NC group (Fig. 7).

In order to further explore the mechanism, a further 6 nude mice were randomly divided into two groups: si-SIRT1 or si-NC (n=3); HL60/C cells transfected with si-SIRT1 or si-NC were subcutaneously injected into nude mice. At day 7, mice were intraperitoneally injected with cytarabine (20 mg/kg, three times a week) for 2 weeks. Tumor growth was measured every other day. The results showed that knockdown of SIRT1 significantly decreased the weight of tumors derived from HL60/C cells in mice (Fig. 8A). Moreover, serum and tumor tissue samples of 6 nude mice were collected, The si-SIRT1 group exhibited decreased SOD activity and increased the MDA content in serum compared with those in the si-NC group (Fig. 8B and C). Meanwhile, SIRT1 knockdown significantly inhibited GPX4 expression in tumor tissues (Fig. 8D). Furthermore, it was observed that the protein expression levels of ACSL4 in tumor tissues were increased in the si-SIRT1 group of mice compared with those in the si-NC group (Fig. 8E). In addition, compared with those in the si-NC group, the protein expression levels of HMGB1 were increased in the cytoplasm and were decreased in the nucleus of HL60/C cells after knockdown of SIRT1 in mice tumor tissues (Fig. 8F). These findings suggested that knockdown of SIRT1 may promote the translocation of HMGB1 from the nucleus to the cytoplasm.

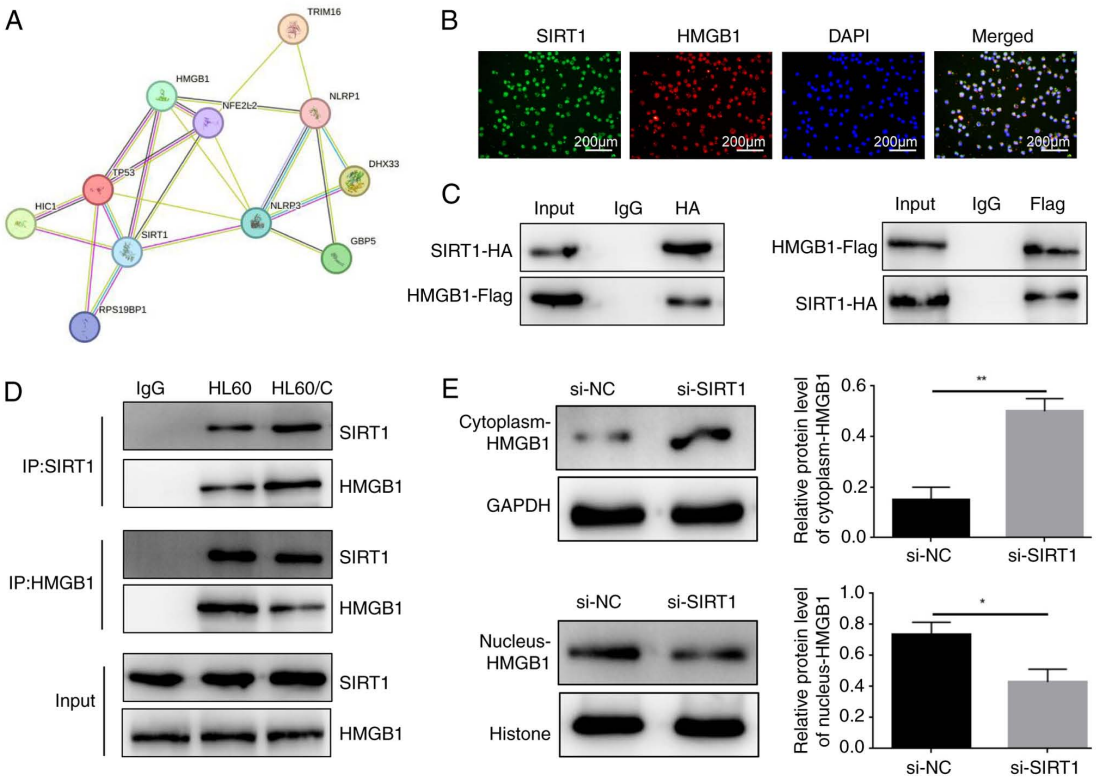

Figure 4. SIRT1 regulates HMGB1 expression and inhibits cytoplasmic translocation of HMGB1. (A) STRING database analysis indicated that SIRT1 may regulate HMGB1 expression. (B) Immunofluorescence staining of SIRT1 and HMGB1 in HL60/C cells. (C) Co-IP with tag analysis of the interaction between SIRT1 and HMGB1 in HL60/C cells. (D) Co-IP analysis of the interaction of SIRT1 and HMGB1 in HL60 and HL60/C cells. (E) Western blot analysis of the levels of HMGB1 in the cytoplasm and nucleus of HL60/C cells after SIRT1 knockdown. *P<0.05, **P<0.01. HL60/C, cytarabine-resistant HL60; HMGB1, high mobility group box-1 protein; IP, immunoprecipitation; NC, negative control; si, small interfering; SIRT1, sirtuin 1.

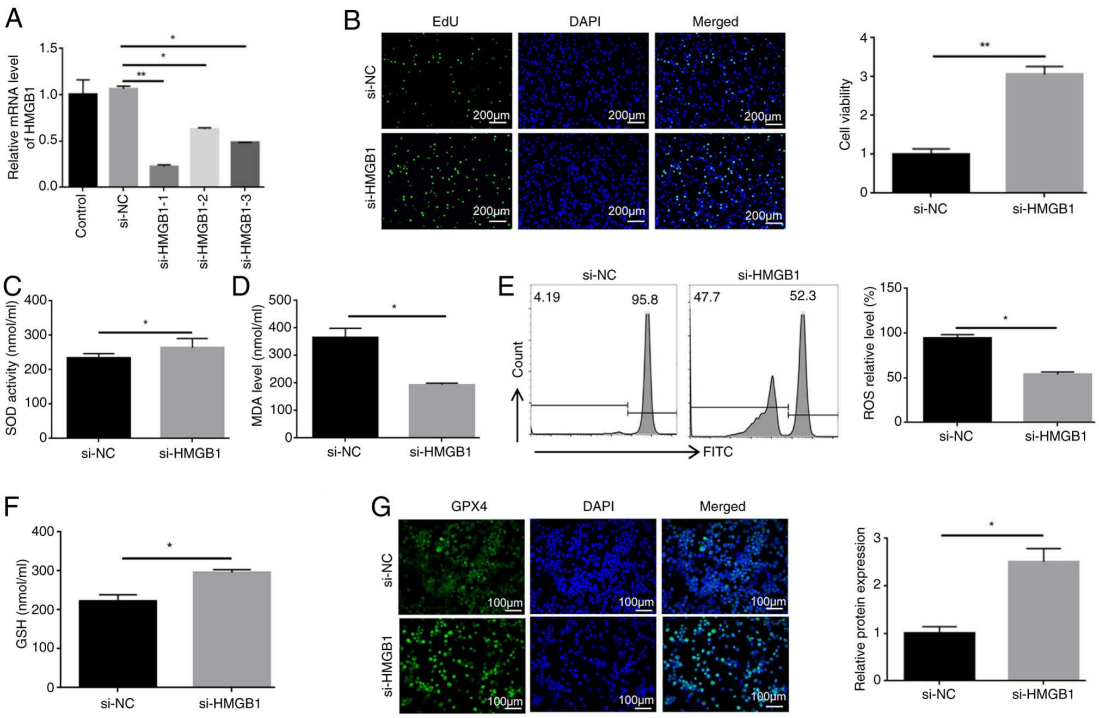

Figure 5. Knockdown of HMGB1 reduces the ferroptosis of HL60/C cells. (A) Reverse transcription-quantitative PCR analysis of the knockdown efficiency of si-HMGB1 sequences. (B) EdU proliferation assay was used to detect the effect of HMGB1 knockdown on the viability of HL60/C cells. ELISAs were used to determine the effect of HMGB1 knockdown on (C) SOD activities and (D) MDA levels in HL60/C cells. (E) Flow cytometry detected the impact of HMGB1 knockdown on ROS levels in HL60/C cells. (F) ELISA was used to detect the levels of GSH in HL60/C cells. (G) Immunofluorescence staining analyzing the effects of HMGB1 knockdown on GPX4 expression in HL60/C cells. *P<0.05, **P<0.01. GPX4, glutathione peroxidase 4; GSH, glutathione; HL60/C, cytarabine-resistant HL60; HMGB1, high mobility group box-1 protein; MDA, malondialdehyde; NC, negative control; ROS, reactive oxygen species; si, small interfering; SOD, superoxide dismutase.

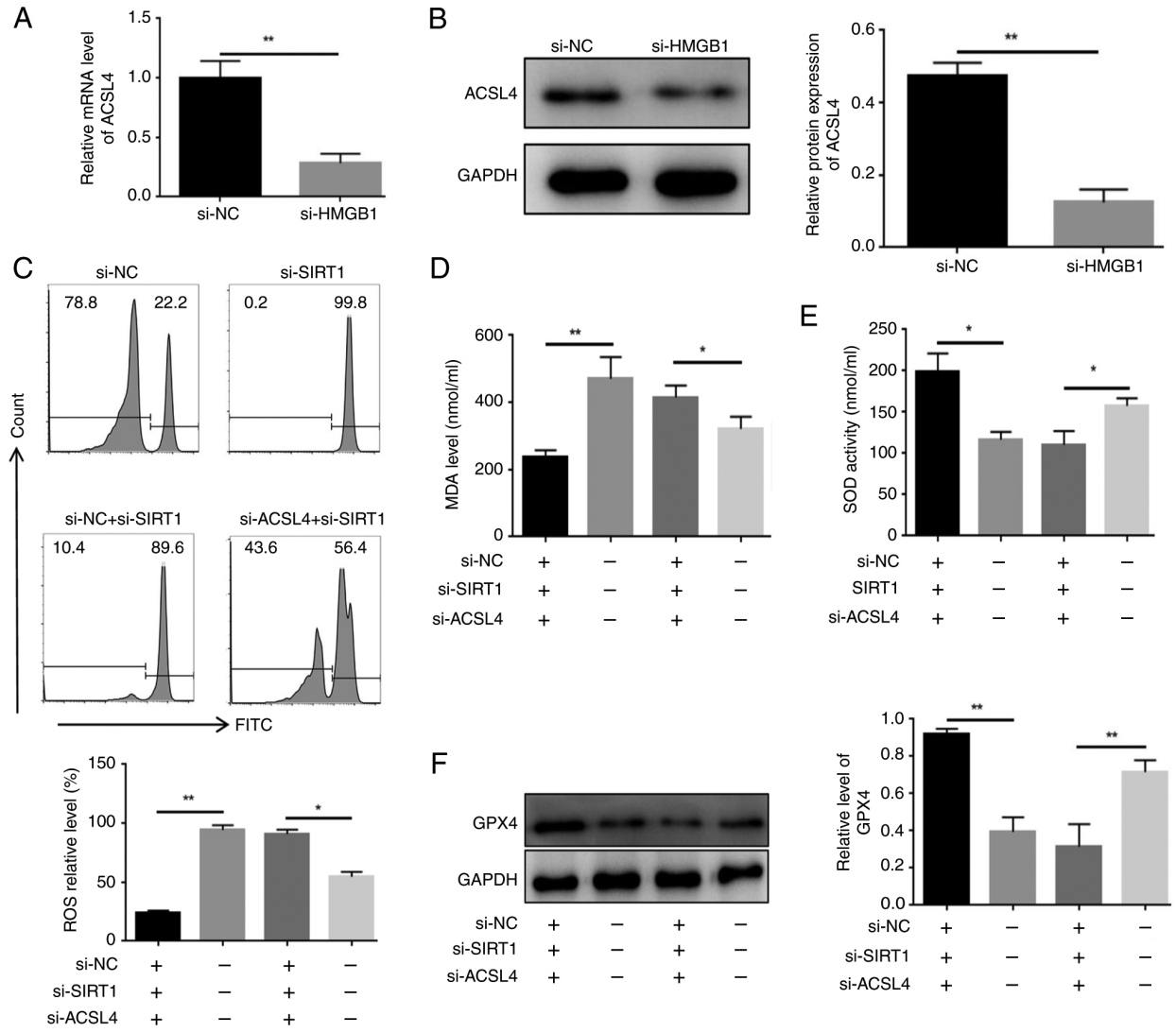

Figure 6. Knockdown of HMGB1 reduces the expression of ACSL4 in HL60/C cells. (A) Reverse transcription-quantitative PCR and (B) western blot analysis of the expression levels of ACSL4 in HL60/C cells with HMGB1 knockdown. (C) Flow cytometry detection of the impact of SIRT1 knockdown and/or ACSL4 knockdown on ROS levels in HL60/C cells. ELISAs were used to examine the effects of SIRT1 knockdown and/or ACSL4 knockdown on (D) MDA and (E) SOD in HL60/C cells. (F) Western blot analysis of the expression levels of GPX4 in HL60/C cells after SIRT1 knockdown and/or ACSL4 knockdown. *P<0.05, **P<0.01. GPX4, glutathione peroxidase 4; HL60/C, cytarabine-resistant HL60; HMGB1, high mobility group box-1 protein; MDA, malondialdehyde; NC, negative control; ROS, reactive oxygen species; si, small interfering; SIRT1, sirtuin 1; SOD, superoxide dismutase.

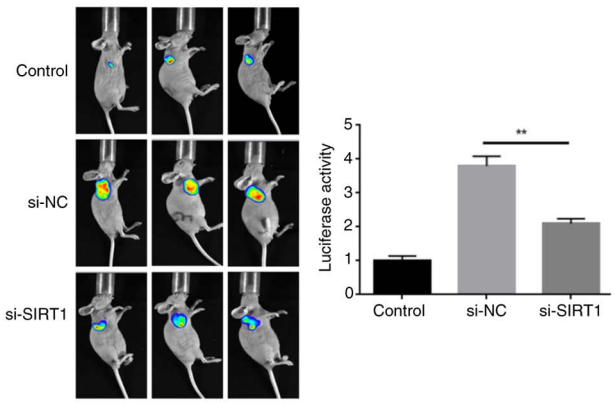

Figure 7. Knockdown of SIRT1 significantly decreases the growth of tumors derived from HL60/C cells in mice. Luciferase activity assay detecting the impact of SIRT1 knockdown on the growth of HL60/C cells in mice. **P<0.01. HL60/C, cytarabine-resistant HL60; NC, negative control; si, small interfering; SIRT1, sirtuin 1.

Discussion

The emergence of drug resistance is an important problem in the treatment of AML. It has been reported that inducing ferroptosis is an important strategy to reduce drug resistance; however, the underlying mechanism remains unclear. The present study revealed that SIRT1 expression was upregulated in cytarabine-resistant leukemia cells. Knockdown of SIRT1 reversed AML drug resistance by promoting ferroptosis. Mechanistically, inhibition of SIRT1 expression could promote the translocation of HMGB1 from the nucleus to the cytoplasm, and thereby enhance ACSL4-mediated ferroptosis (Fig. 8G).

Ferroptosis is a form of cell death different from apoptosis, necrosis and autophagy. It has been shown that ferroptosis serves a key role in tumor suppression, thus providing new opportunities for cancer treatment (9). The development of drug resistance to cancer treatments remains a major challenge, and some preclinical and clinical studies have focused on overcoming drug

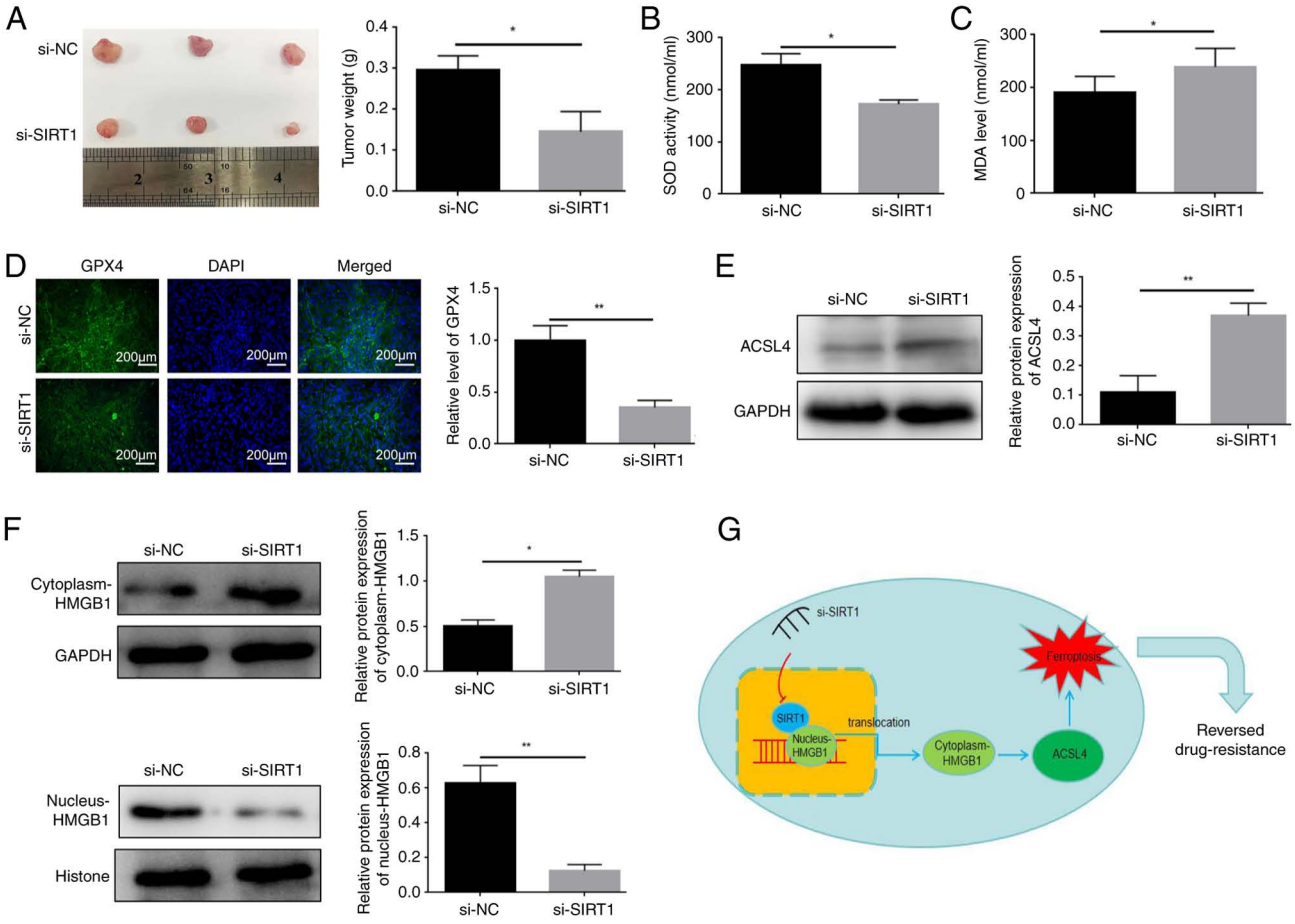

Figure 8. Knockdown of SIRT1 blocks the growth of HL60/C cells *in vivo*. HL60/C cells transfected with si-SIRT1 or si-NC were subcutaneously injected into nude mice for 2 weeks. (A) Images of tumors (units: Inches) and tumor weight (n=3). ELISAs were used to determine (B) SOD and (C) MDA in tumors from the si-NC and si-SIRT1 groups. (D) Immunofluorescence staining analyzing the expression of GPX4 in tumors from the si-NC and si-SIRT1 groups. (E) Western blot analysis of the expression levels of ACSL4 in tumors from the si-NC and si-SIRT1 groups. (F) Western blot analysis of the cytoplasmic and nuclear levels of HMGB1 in the si-NC and si-SIRT1 groups. (G) Mechanism by which SIRT1 can decrease ferroptosis and increased drug resistance of leukemia cells. *P<0.05, **P<0.01. HL60/C, cytarabine-resistant HL60; HMGB1, high mobility group box-1 protein; MDA, malondialdehyde; NC, negative control; si, small interfering; SIRT1, sirtuin 1; SOD, superoxide dismutase.

resistance (3,4). Notably, ferroptosis has been shown to be associated with cancer treatment resistance and inducing ferroptosis may reverse resistance (21-23). Previous research has demonstrated that erastin, a ferroptosis inducer, can improve the sensitivity of leukemia cells to cytarabine (12); however, the underlying mechanism remains unclear. GPX4 is a crucial regulator of ferroptosis, which converts lipid hydroperoxides by reducing GSH, whereas SOD functions as an antioxidant that removes excessive ROS and lipid oxidation (24,25). Prior research has shown that as ferroptosis progresses, lipid peroxidation generates elevated levels of ROS and MDA (25). In the present study, knockdown of SIRT1 could enhance GPX4 expression and SOD activity, whereas it decreased ROS and MDA content in HL60/C cells. These findings suggested that SIRT1 knockdown could reverse cytarabine resistance in AML by enhancing ferroptosis.

A growing body of evidence has established that HMGB1 serves a significant role in multiple drug resistance, including resistance to thiopurines, 5-fluorouracil and cytarabine (3). Upregulation of HMGB1 expression in erastin-treated HL60 cells expressing $NRAS^{Q61L}$ has previously been demonstrated (26). As expected, the present results showed that silencing HMGB1 increased the levels of GPX4 and SOD but decreased the levels of MDA and ROS in HL60/C cells, which was consistent with previous findings (6). These results provide evidence supporting the role of HMGB1 in the process of ferroptosis in cytarabine-resistant leukemia cells. HMGB1 is normally localized in the nucleus of cells, but is released extracellularly when the body is exposed to stimuli or damage (27,28). HMGB1 can function as both a nuclear DNA-binding molecule and a secreted protein. The localization and biological function of HMGB1 are determined by its post-translational modification (29). It has previously been shown that treatment with chemotherapeutic drugs can promote the translocation of HMGB1 from the nucleus to the cytoplasm (30). The present study observed an increase in the cytoplasmic levels of HMGB1 and a decrease in its nuclear level in the si-SIRT1 group compared with in the si-NC group. While SIRT1 has been identified as serving an important role in cytarabine resistance, the underlying mechanism remains partially understood (17,31). A previous study reported that SIRT1 could inhibit HMGB1 translocation to the cytoplasm and the expression of inflammatory cytokines, attenuating bone cancer pain symptoms in mice (32). Furthermore, cytoplasmic translocation of HMGB1 has been detected in high glucose-treated mesangial cells, which can

increase positive regulators of ferroptosis, such as ACSL4, and enhance ferroptosis (33). In the present study, the results showed that knockdown of SIRT1 elevated the translocation of HMGB1 from the nucleus to the cytoplasm, and increased the expression levels of ACSL4 *in vivo*.

In conclusion, the present study demonstrated that induction of ferroptosis by SIRT1 knockdown may alleviate cytarabine resistance in AML by activating the HMGB1/ACSL4 pathway. Therefore, targeting SIRT1 may hold promise as a strategy to overcome cytarabine resistance in AML.

Acknowledgements

Not applicable.

Funding

This work was supported by the Doctoral Start-up Fund of Natural Science Foundation of Guangdong Province under Grant (grant no. 2016A030310161) and the National Natural Science Foundation for Young Scientists of China (grant no. 82100181).

Availability of data and materials

The data generated in the present study may be requested from the corresponding author.

Authors' contributions

QK and HC conceived and designed the experiments. QL and YT performed the experiments. XL, XL, YC and YL analyzed and interpreted the data. QK and HC confirm the authenticity of all the raw data, QK wrote the paper. All authors read and approved the final version of the manuscript.

Ethics approval and consent to participate

All experiments were approved by the Animal Ethics Committee of the Guangzhou Seyotin Biotechnology Co., Ltd. (approval no. SYT20203010). The requirement to obtain additional approval from the authors' own institution for the outsourcing of the animal experiments was waived by the ethics committee of the Third Affiliated Hospital of Sun Yat-sen University (Guangzhou, China).

Patient consent for publication

Not applicable.

Competing interests

The authors declare that they have no competing interests.

References

1. Pelcovits A and Niroula R. Acute myeloid leukemia: A review. R I Med J 103: 38-40, 2013.
2. Ganesan S, Mathews V and Vyas N: Microenvironment and drug resistance in acute myeloid leukemia: Do we know enough? Int J Cancer 150: 1401-1411, 2022.
3. Heuser M, Ofran Y, Boissel N, Brunet Mauri S, Craddock C, Janssen J, Wierzbowska A, Buske C and ESMO Guidelines Committee. Electronic address: clinicalguidelines@esmo.org: Acute myeloid leukaemia in adult patients: ESMO Clinical Practice Guidelines for diagnosis, treatment and follow-up. Ann Oncol 31: 697-712, 2020.
4. Cros E, Jordheim L, Dumontet C and Galmarini CM: Problems related to resistance to cytarabine in acute myeloid leukemia. Leuk Lymphoma 45: 1123-1132, 2004.
5. Liu L, Yang M, Kang R, Wang Z, Zhao Y, Yu Y, Xie M, Yin X, Livesey KM, Lotze MT, *et al*: HMGB1-induced autophagy promotes chemotherapy resistance in leukemia cells. Leukemia 25: 23-31, 2011.
6. Ye F, Chai W, Xie M, Yang M, Yu Y, Cao L and Yang L: HMGB1 regulates erastin-induced ferroptosis via RAS-JNK/p38 signaling in HL-60/NRAS^{Q61L} cells. Am J Cancer Res 9: 730-739, 2019.
7. Krynetskaia N, Xie H, Vucetic S, Obradovic Z and Krynetskiy E: High mobility group protein B1 is an activator of apoptotic response to antimetabolite drugs. Mol Pharmacol 73: 260-269, 2008.
8. Dixon SJ, Lemberg KM, Lamprecht MR, Skouta R, Zaitsev EM, Gleason CE, Patel DN, Bauer AJ, Cantley AM, Yang WS, *et al*: Ferroptosis: An iron-dependent form of nonapoptotic cell death. Cell 149: 1060-1072, 2012.
9. Zhang C, Liu X, Jin S, Chen Y and Guo R: Ferroptosis in cancer therapy: A novel approach to reversing drug resistance. Mol Cancer 21: 47, 2022.
10. Hong T, Lei G, Chen X, Li H, Zhang X, Wu N, Zhao Y, Zhang Y and Wang J: PARP inhibition promotes ferroptosis via repressing SLC7A11 and synergizes with ferroptosis inducers in BRCA-proficient ovarian cancer. Redox Biol 42: 101928, 2021.
11. Liu Q and Wang K: The induction of ferroptosis by impairing STAT3/Nrf2/GPx4 signaling enhances the sensitivity of osteosarcoma cells to cisplatin. Cell Biol Int 43: 1245-1256, 2019.
12. Yu Y, Xie Y, Cao L, Yang L, Yang M, Lotze MT, Zeh HJ, Kang R and Tang D: The ferroptosis inducer erastin enhances sensitivity of acute myeloid leukemia cells to chemotherapeutic agents. Mol Cell Oncol 2: e1054549, 2015.
13. Shen P, Deng X, Chen Z, Ba X, Qin K, Huang Y, Li T, Yan J and Tu S: SIRT1: A potential therapeutic target in autoimmune diseases. Front Immunol 12: 779177, 2021.
14. Kim TH, Young SL, Sasaki T, Deaton JL, Schammel DP, Palomino WA, Jeong J-W and Lessey BA: Role of SIRT1 and progesterone resistance in normal and abnormal endometrium. J Clin Endocrinol Metab 107: 788-800, 2022.
15. Liu Z, Li C, Yu C, Chen Z, Zhao C and Ye L: TSPYL2 reduced gefitinib resistance and DNA damage repair via suppressing SIRT1-mediated FOXO3 deacetylation. Future Med Chem 14: 407-419, 2022.
16. Zhu X, Su Q, Xie H, Song L, Yang F, Zhang D, Wang B, Lin S, Huang J, Wu M and Liu T: SIRT1 deacetylates WEE1 and sensitizes cancer cells to WEE1 inhibition. Nat Chem Biol 19: 585-595, 2023.
17. Jin Y, Cao Q, Chen C, Du X, Jin B and Pan J: Tenovin-6-mediated inhibition of SIRT1/2 induces apoptosis in acute lymphoblastic leukemia (ALL) cells and eliminates ALL stem/progenitor cells. BMC Cancer 15: 226, 2015.
18. Zhao Z, Li G, Wang Y, Li Y, Xu H, Liu W, Hao W, Yao Y and Zeng R: Cytoplasmic HMGB1 induces renal tubular ferroptosis after ischemia/reperfusion. Int Immunopharmacol 116: 109757, 2023.
19. Gu L, Zhang G and Zhang Y: A novel method to establish glucocorticoid resistant acute lymphoblastic leukemia cell lines. J Exp Clin Cancer Res 38: 269, 2019.
20. Livak KJ and Schmittgen TD: Analysis of relative gene expression data using real-time quantitative PCR and the 2(-Delta Delta C(T)) method. Methods 25: 402-408, 2001.
21. Mandke P and Vasquez KM: Interactions of high mobility group box protein 1 (HMGB1) with nucleic acids: Implications in DNA repair and immune responses. DNA Repair (Amst) 83: 102701, 2019.
22. Luo L, Wang S, Chen B, Zhong M, Du R, Wei C, Huang F, Kou X, Xing Y and Tong G: Inhibition of inflammatory liver injury by the HMGB1-A box through HMGB1/TLR-4/NF-kappaB signaling in an acute liver failure mouse model. Front Pharmacol 13: 990087, 2022.

23. Ling VY, Straube J, Godfrey W, Haldar R, Janardhanan Y, Cooper L, Bruedigam C, Cooper E, Shirazi PT, Jacquelin S, *et al*: Targeting cell cycle and apoptosis to overcome chemotherapy resistance in acute myeloid leukemia. Leukemia 37: 143-153, 2023.
24. Zhang H, Liu L, Chen L, Liu H, Ren S and Tao Y: Long noncoding RNA DANCR confers cytarabine resistance in acute myeloid leukemia by activating autophagy via the miR-874-3P/ATG16L1 axis. Mol Oncol 15: 1203-1216, 2021.
25. Chromik J, Safferthal C, Serve H and Fulda S: Smac mimetic primes apoptosis-resistant acute myeloid leukaemia cells for cytarabine-induced cell death by triggering necroptosis. Cancer Lett 344: 101-109, 2014.
26. Yang WS and Stockwell BR: Ferroptosis: Death by lipid peroxidation. Trends Cell Biol 26: 165-176, 2016.
27. Wang X, Wang Z, Cao J, Dong Y and Chen Y: Melatonin alleviates acute sleep deprivation-induced memory loss in mice by suppressing hippocampal ferroptosis. Front Pharmacol 12: 708645, 2021.
28. Zheng H, Chen JN, Yu X, Jiang P, Yuan L, Shen HS, Zhao LH, Chen PF and Yang M: HMGB1 enhances drug resistance and promotes in vivo tumor growth of lung cancer cells. DNA Cell Biol 35: 622-627, 2016.
29. Splichal I, Donovan SM, Jenistova V, Splichalova I, Salmonova H, Vlkova E, Bunesova VN, Sinkora M, Killer J, Skrivanova E and Splichalova A: High mobility group box 1 and TLR4 signaling pathway in gnotobiotic piglets colonized/infected with *L. amylovorus*, *L. mucosae*, *E. coli* Nissle 1917 and S. Typhimurium. Int J Mol Sci 20: 6294, 2019.
30. Li J, Zhou W, Mao Q, Gao D, Xiong L, Hu X, Zheng Y and Xu X: HMGB1 promotes resistance to doxorubicin in human hepatocellular carcinoma cells by inducing autophagy via the AMPK/mTOR signaling pathway. Front Oncol 11: 739145, 2021.
31. Bhanot H, Weisberg EL, Reddy MM, Nonami A, Neuberg D, Stone RM, Podar K, Salgia R, Griffin JD and Sattler M: Acute myeloid leukemia cells require 6-phosphogluconate dehydrogenase for cell growth and NADPH-dependent metabolic reprogramming. Oncotarget 8: 67639-67650, 2017.
32. Chen X, Chen C, Fan S, Wu S, Yang F, Fang Z, Fu H and Li Y: Omega-3 polyunsaturated fatty acid attenuates the inflammatory response by modulating microglia polarization through SIRT1-mediated deacetylation of the HMGB1/NF-kappaB pathway following experimental traumatic brain injury. J Neuroinflammation 15: 116, 2018.
33. Wu Y, Zhao Y, Yang HZ, Wang YJ and Chen Y: HMGB1 regulates ferroptosis through Nrf2 pathway in mesangial cells in response to high glucose. Biosci Rep 41: BSR20202924, 2021.